Multicycle Dynamics of Fault Systems and Static and Dynamic Triggering of Earthquakes

L.M. Olsen-Kettle[1,2], D. Weatherley[1], L. Gross[1] and H.-B. Mühlhaus[1]

1. Earth Systems Science Computational Centre,The University of Queensland, St Lucia QLD 4072, Australia.
2. Corresponding author. Email: lkettle@esscc.uq.edu.au

ABSTRACT

Dynamic simulations of rupture propagation and multiple earthquake cycles for varying fault geometries are presented. We investigate the role of both dynamic and static stress changes on earthquake triggering. Dynamic stress triggering of earthquakes is caused by the passage of seismic waves, whereas static stress triggering is due to net slippage on a fault resulting from an earthquake. Static stress changes represented by a Coulomb failure function and its relationship to seismicity rate change is a relatively well-known mechanism, whereas the physical origin of dynamic triggering remains one of the least understood aspects of earthquake nucleation. We investigate these mechanisms by analysing seismicity patterns with varying fault separation, geometry and with and without dynamic triggering present.

Keywords: dynamics of earthquake rupture, interacting fault systems, dynamic and static stress triggering, wave propagation, synthetic seismicity studies

1 INTRODUCTION

Earthquake triggering is the process by which stress changes associated with an earthquake can induce or retard seismic activity in the surrounding region. There is mounting evidence to suggest that small, sudden stress changes due to earthquakes

can cause large changes in seismicity rates. However, in most probabilistic seismic hazard assessments there is no feature that can reflect or reproduce such observations (Stein, 1999). Earthquake interaction is a fundamental feature of seismicity leading to earthquake sequences, clustering, aftershock distributions and the quiescence of broad normally active regions following large earthquakes.

Several kinds of earthquake interaction can affect seismicity rates. Calculations of static Coulomb stress (shear stress plus normal stress multiplied by the coefficient of friction) transfer have proven to be a powerful tool in explaining many near-field aftershock distributions (usually up to 1-2 fault lengths) (Freed, 2005). Dynamic stress changes due to the passage of seismic waves cause transient dynamic stress oscillations, and in contrast, attenuate more slowly and thus dominate at large distances, depending on earthquake magnitude and directivity (Stein, 1999)).

In this numerical study we generate and analyse slip time histories for parallel fault models with varying fault geometries and separations. We compare the seismicity rates generated at the two faults with varying separation between them, and also for cases where the static Coulomb stress is decreased or increased on fault two due to net slippage on fault one (and vice versa). In addition we compare the slip time histories generated for the parallel fault models where earthquake interaction is present, with the single fault slip time histories for the same tectonic loading conditions and frictional properties at the faults. This allows us to verify that static stress shadowing or triggering, and dynamic triggering do have an effect on the observed seismicity rates in comparison to the seismicity rate produced without earthquake interactions present. This is a feature which is impossible to study in naturally occurring earthquake sequences. We also test the relative importance of static over dynamic triggering and present results which distinguish between earthquake triggering where only static stress triggering is present and where both mechanisms can contribute. To do this we compare seismicity rates produced with and without dynamic triggering present. Removing the dynamic triggering mechanism is achieved by clamping the fault not slipping initially so that it is unable to fail while the other fault is slipping.

2 NUMERICAL RESULTS

The 2D elastic wave equation is solved using the finite element method. The tractions at the fault interface are represented using the penalty method and elasto-plasticity theory (Olsen-Kettle et al., 2007). We employ a very strongly slip-weakening frictional law, which was used because it reproduces more realistic seismicity characteristics. Rice (1993) showed that spatially discrete models where the mesh elements are oversized (with respect to the critical length scale that is implied by the frictional law) can produce more spatially-temporally complex slip events. For this reason we also used oversized mesh elements with respect to our frictional law in our model. Tectonic loading was implemented by shearing the domain boundaries tangential to the fault, and compressing the domain boundaries normal to the fault. Reloading between events was achieved by continuing to shear the boundaries tangential to

fault until one point on the fault reaches failure and either an earthquake or creep event results.

In all figures of slip time history we plot the tectonic time (proportional to the shearing strain applied) vs. the fault position. Regions on the fault which have undergone any plastic slip no matter how small are plotted as red lines (in the case that more than one fault element fails) or dots (for small creep events where only one fault element fails). Small creep events are generally single points on these plots with slips less (can be much less) than 1mm. In these figures we also identify the rupture nucleation point in green and the point with maximum slip in blue for each earthquake or creep event.

2.1 SINGLE FAULT SLIP TIME HISTORIES

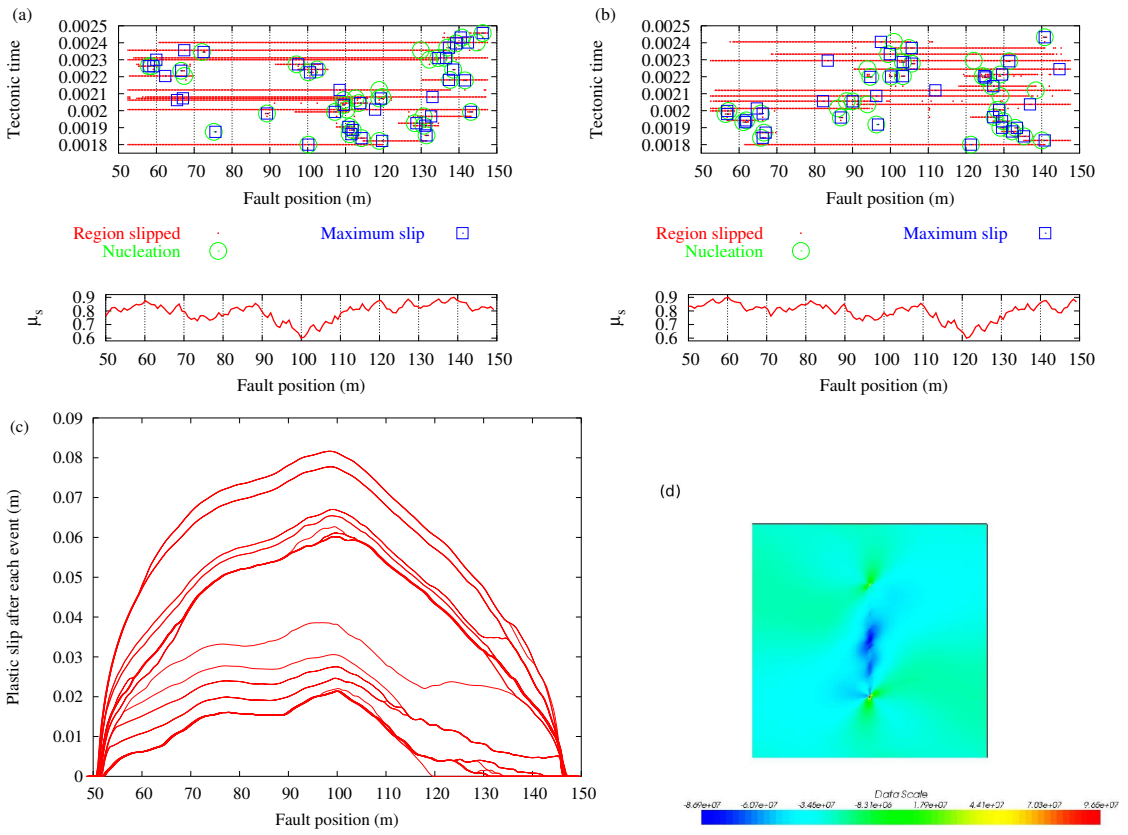

Figure 1: Slip time history plots generated for homogeneous faults with different distributions of μ_s (shown in inset below) in (a) and (b). Total plastic slip accumulated after each event in (c) and Coulomb stress after 20 earthquakes in (d), for distribution of μ_s in (a).

Figure 1 shows the slip time histories for single fault simulations with different fractal distributions of μ_s in (a) and (b). We can observe that for the first earthquake event (at tectonic time of 0.0018) the rupture nucleation and maximum slip occurs at a fault position of 100m in (a) and close to 120m in (b). These points on the faults correspond to the weakest points for faults (a) and (b), where their static coefficient

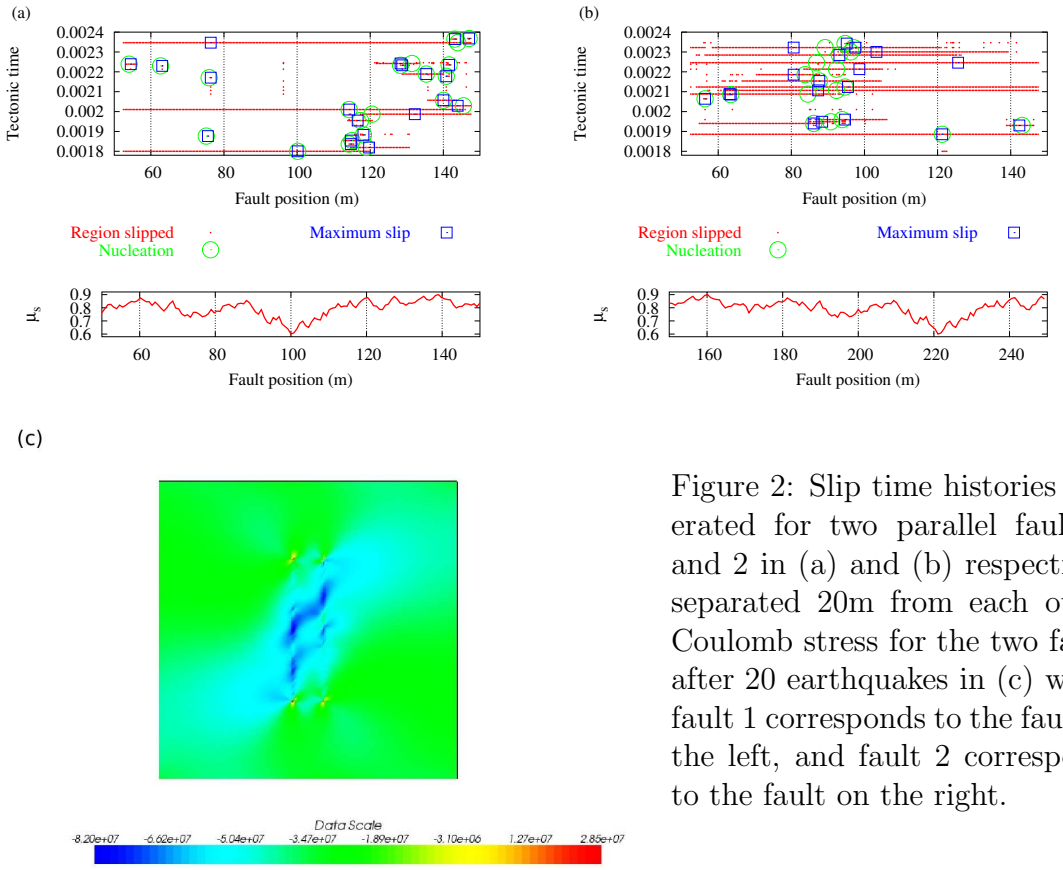

Figure 2: Slip time histories generated for two parallel faults 1 and 2 in (a) and (b) respectively separated 20m from each other. Coulomb stress for the two faults after 20 earthquakes in (c) where fault 1 corresponds to the fault on the left, and fault 2 corresponds to the fault on the right.

of friction (μ_s) reaches its minimum value. Rupture nucleates at these points and propagates bilaterally along the faults. In both cases the rupture propagates all the way to the end at 50m (in the left direction), whereas in the right direction the rupture is terminated before it reaches the end at 150m. Rupture is terminated earlier in this direction because μ_s is on average higher in this direction and can "lock" the fault at particularly high values of μ_s.

Figures 1(a) and (b) show realistic aftershock sequences where clusters of aftershocks form in regions close to where the fault stopped slipping in the last big earthquake event. Figure 1(c) shows the accumulated plastic slip along the fault after each event. This shows the richly complex slip our fault model produces with over-sized mesh elements. It can be compared to Figure 6(a) in Rice (1993). Figure 1(d) shows the Coulomb stress calculated after 20 earthquakes. We calculate the Coulomb stress over the whole domain using:

$$\text{Coulomb stress} = |\sigma \,.\, \boldsymbol{n} \,.\, \boldsymbol{\tau}| + \mu_{fri}\sigma \,.\, \boldsymbol{n} \,.\, \boldsymbol{n}.$$

We show these figures in order to compare the seismicity patterns generated with only one fault with our two-fault models where both Coulomb stress effects and dynamic triggering are present.

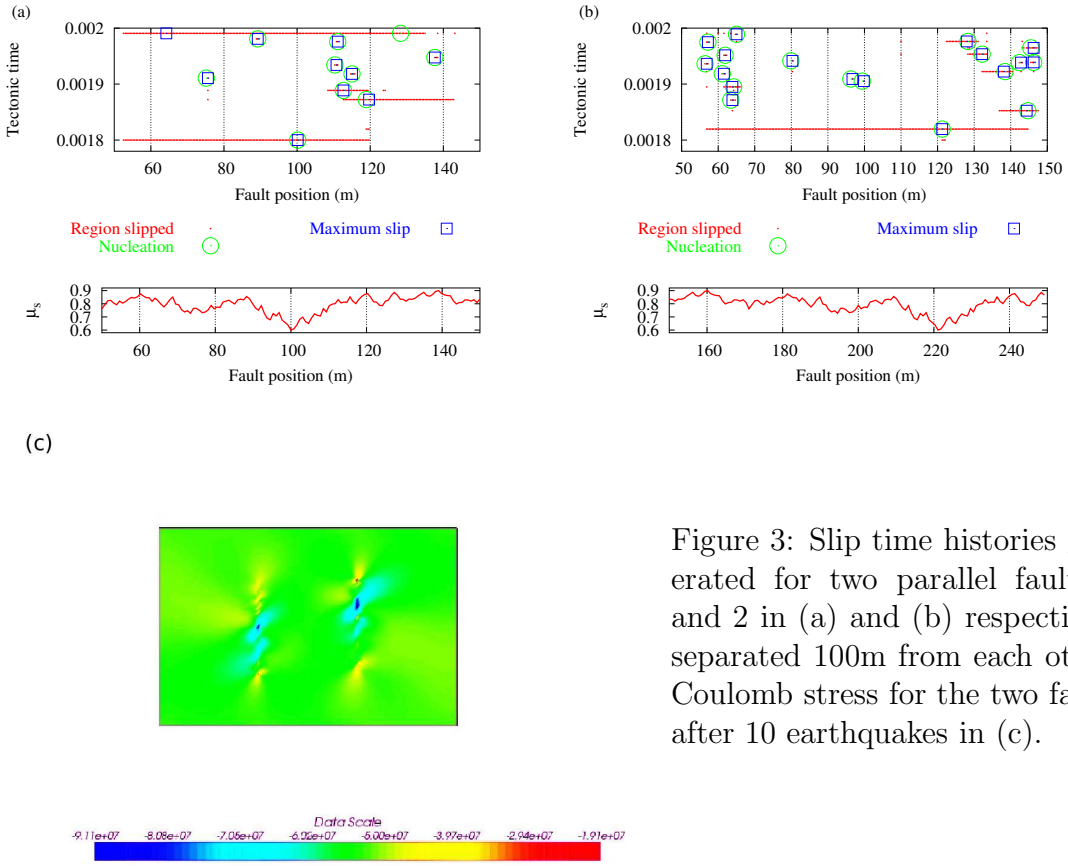

Figure 3: Slip time histories generated for two parallel faults 1 and 2 in (a) and (b) respectively separated 100m from each other. Coulomb stress for the two faults after 10 earthquakes in (c).

2.2 TWO-FAULT MODELS WITH AND WITHOUT DYNAMIC TRIGGERING PRESENT

Please note that in the following two-fault models we always define fault 1 to be on the left of the domain and fault 2 on the right. In Figure 2 we show slip time histories for two parallel faults separated 20m from each other. This plot was produced with dynamic stress triggering present, where both faults can fail at the same time. Figure 2(a) clearly shows that the earthquakes occurring on fault 2 lead to suppression of earthquake activity (stress "shadowing") at fault 1 when compared with the single fault seismicity rate in Figure 1(a). In Figure 2(b) we observe that some creep occurs on fault 2 due to the first earthquake rupture initiated at fault 1 (when tectonic time = 0.0018). We show later in Figure 5 that dynamic triggering by seismic waves can also cause large earthquakes (in addition to creep events) at nearby faults, depending on that fault's critical state and the rupture directivity effects.

We were also able to investigate the importance of dynamic triggering by running the same simulations with a larger separation (100m) in Figures 3 and 4. Figures 3 and 4 show that there is indeed some difference in the slip time histories generated at larger distances with and without dynamic stress triggering present. Simulations without dynamic triggering were achieved by modifying our multicycle code so that the fault which is not slipping initially is "clamped shut" during the rupture and cannot slip until after the earthquake rupture has finished and all seismic waves

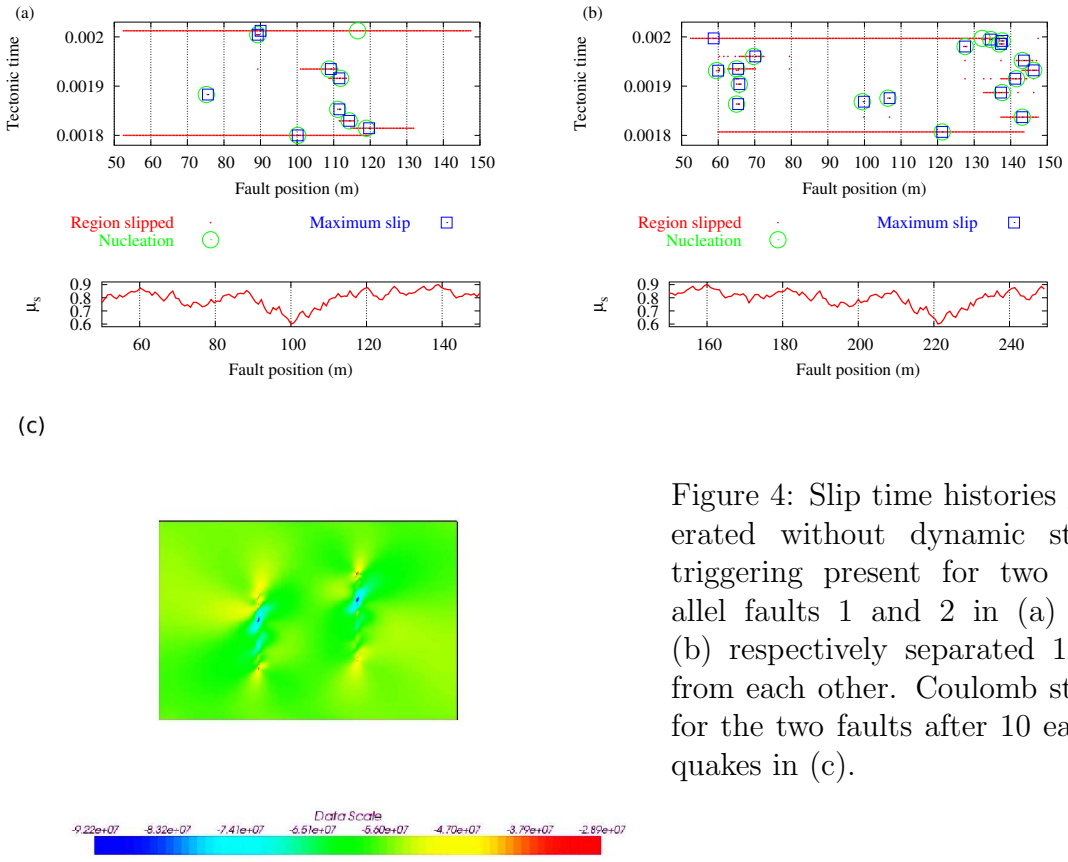

(c)

Figure 4: Slip time histories generated without dynamic stress triggering present for two parallel faults 1 and 2 in (a) and (b) respectively separated 100m from each other. Coulomb stress for the two faults after 10 earthquakes in (c).

have disappeared. These preliminary simulations give us confidence that dynamic stress triggering is important at large distances and needs to be investigated more thoroughly with longer simulation times as well as larger distances. Figures 3(a) and (b) show a greater number of creep events occurring than the corresponding plots in Figure 4 without dynamic stress triggering present.

Figure 5 shows the Coulomb stress calculated at different times during earthquake rupture which began at fault 1, for a more complex geometry where the faults are parallel but at different locations in y. We observe that in Figure 5(c) that the seismic waves traveling from fault 1 have dynamically triggered a second event in fault 2.

3 CONCLUSIONS AND FUTURE DIRECTIONS

Of the two mechanisms we study, dynamic triggering is the least understood. Generally seismologists can only attribute events occurring due to dynamic triggering based on distance from the fault or rupture directivity effects (as dynamic stress increases by an order of magnitude in the direction of rupture (Stein, 1999)). Another difference between static and dynamic triggering of earthquakes is that dynamic stresses are transient and oscillate such that they are positive everywhere at some point in time. We shed some light on near-field dynamic triggering and show it is

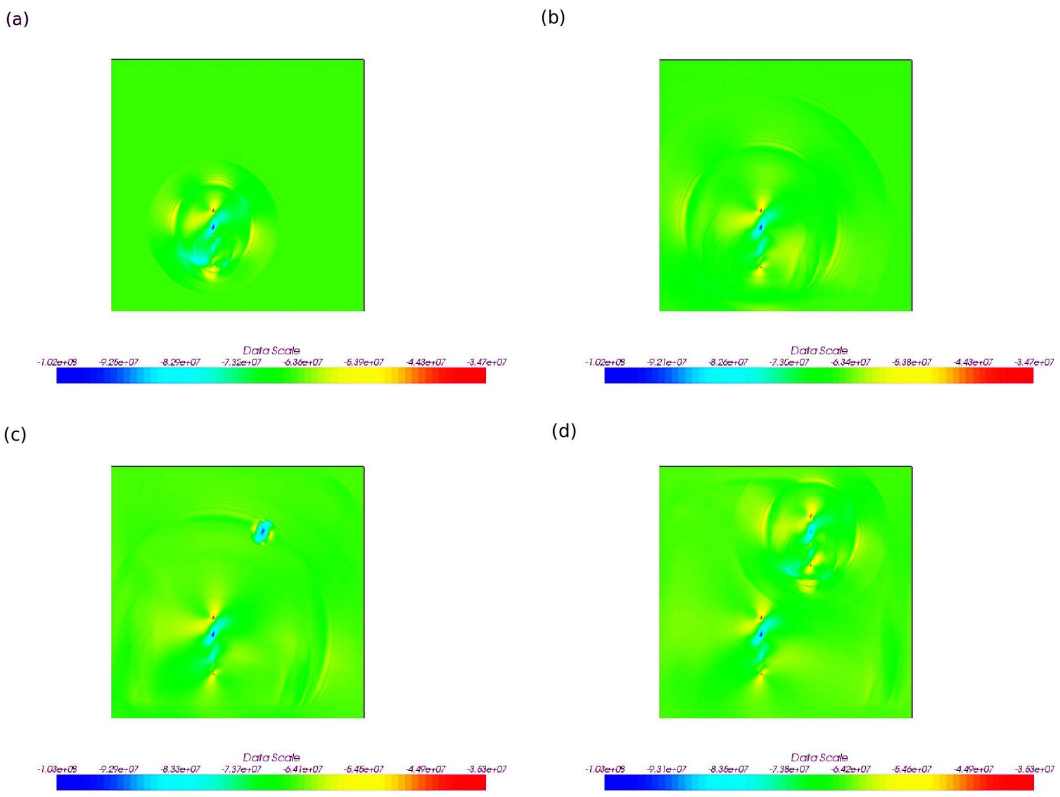

Figure 5: Coulomb stress in (a)-(d) at time intervals of 0.0065s during during the first earthquake event for parallel faults separated approximately 85m from each other. Plot (c) shows that dynamic stress triggering at fault 2 has occurred due to the earthquake event at fault 1.

also important. We have also been successful in verifying that static Coulomb stress changes also affect seismicity patterns and lead to regions of stress "shadows" and "triggers".

Resolving the issue of delayed triggering is also important since most remotely triggered seismicity occurs after a delay (seconds to weeks) in contrast to what one might expect with dynamic triggering - no delay. Delayed earthquake triggering can be explained by a variety of time-dependent stress transfer mechanisms, such as visco-elastic relaxation, poroelastic rebound, afterslip, or by reductions in fault friction (Freed, 2005). The latter two terms can be related to dynamic triggering as it has been proposed that dynamic transient stresses may initiate a time-dependent acceleration to failure process. We have shown in these calculations that dynamic triggering does affect the seismicity patterns (and the number of small creep events) produced. Future work will involve simulating longer earthquake sequences, larger fault separations and more complex fault geometries in order to study the mechanisms of delayed triggering more thoroughly.

References

Freed, A. M. (2005). "Earthquake triggering by static, dynamic and postseismic stress transfer", *Annual Review of Earth and Planetary Sciences*, Vol. 33, pp. 335–367.

Olsen-Kettle, L. M., D. Weatherley, E. Saez, L. Gross, H. B. Mühlhaus, and H. L. Xing (2007). "Analysis of slip-weakening frictional laws and their implications on the scaling, asymmetry and mode of dynamic rupture on homogeneous and bi-material interfaces", submitted to Journal of Geophysical Research.

Rice, J. R. (1993). "Spatio-temporal complexity of slip on a fault", *Journal of Geophysical Research*, Vol. 98, pp. 9885–9907.

Stein, R. S. (1999). "The role of stress transfer in earthquake occurrence", *Nature*, Vol. 402, pp. 605–609.